ACS APPLIED POLYMER MATERIALS

Article

Cite This: ACS Appl. Polym. Mater. 2019, 1, 1624−1633

pubs.acs.org/acsapm

Network of Polyaniline Nanotubes for Wastewater Treatment and Oil/Water Separation

Sanjoy Mondal, Utpal Rana, Puspendu Das, and Sudip Malik*

School of Applied and Interdisciplinary Sciences (Formerly Polymer Science Unit), Indian Association for the Cultivation of Science, , 2A & 2B Raja S.C. Mullick Road., Jadavpur, Kolkata 700032, India

Supporting Information

ABSTRACT: Polyaniline (PANI) nanofibers have been developed by an *in situ* polymerization technique using three different aromatic carboxylic acids as dopant. All dopants have the same aromatic core containing different numbers of carboxylic acid groups. Four (B4CA), three (B3CA), and two (B2CA) carboxylic acid functionalized organic acids have been selected as a dopant for polymerization of aniline in the presence of ammonium persulfate and the corresponding polyaniline composites are named as B4CAP, B3CAP, and B2CAP respectively. With increasing number of −COOH groups in the dopant, the aspect ratio of the fiber increases. Interestingly, all composites revealing nanotubes have shown very good adsorbing behavior toward water-soluble anionic dyes and dye uptake capacity varies with the aspect ratio of the nanofibers. The maximum dye adsorption efficiency achieved for the B4CAP matrix is ∼300 mg/g toward indigo carmine dye in aqueous solution. The dye uptake ability also depends on the size as well as the charge of the dye molecule. Interestingly, PANI hollow nanotubes show good recyclability with several times by simple washing with diluted ammonia and acid solution. By taking advantage of hydrophilicity, polyaniline composites are subsequently employed to the oil/water separation. Polyaniline composites are able to separate different oil/water mixtures in a single-unit operation with >98% separation efficiency.

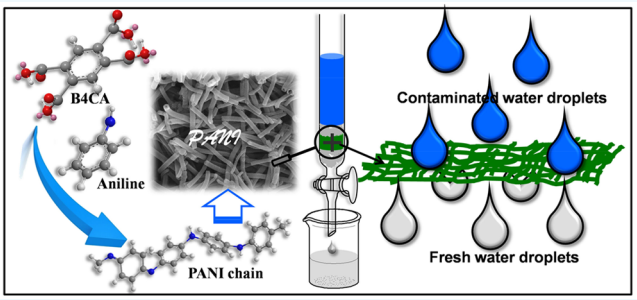

KEYWORDS: *polyaniline, nanotube, adsorption, aspect ratio, recyclability, oil/water separation*

1. INTRODUCTION

Water pollution by toxic dye is a serious environmental issue throughout the world today.[1−4] Many industries like textile, printing, leather, paper, etc. release a large amount of colored effluent to wastewater. All organic dyes that are toxic and nonbiodegradable cause several serious human health problems.[1,5] Hence, carcinogenic dyes need to be removed from industrial wastewater to solve ecological, biological, and environmental problems. To remove hazardous dyes from wastewater, many techniques have been developed, like chemical, physical, biological, etc. Among them, the physical adsorption technique is considered one of the most effective methods due to its easy handling, high efficiency, and simplicity.[6−8] Several efficient adsorbents such as polymers,[9,10] supramolecular gel,[11,12] metal−organic frameworks (MOF),[13] graphene or graphene/metal oxide composite,[14] activated carbon,[15] metal oxide,[16] CNTs,[17] etc. have been used for organic dye adsorption from industrial wastewater. However, the design of an efficient adsorbent is still undergoing challenge in the sense of product cost, eco-friendliness, easy disposal, and reusability for the separation of toxic dye.

Water is polluted not only by toxic dyes but also contaminated by different kinds of industrial waste oils, lubricants, etc. This kind of water pollution affects the lifestyle of animals, birds, human beings, and even whole ecosystems. At this vital situation, people have already prepared many porous, polymeric, thin film membranes, gels, and sponge-based materials for oil separation from water.[18,19] However, several limitations are still present in materials and techniques, in terms of efficiency, low environmental and thermal stability, reusability, mechanical stability, high production cost of materials, low toxicity, etc. There is room for improvement, with respect to loading percentage, cost, stability, and reusability. Therefore, preparation of material that separates dye from wastewater as well as oil from oil/water mixtures is important to solve environmental problems.

It is well established that various synthetic polymers as well as natural polymers are widely used as an efficient adsorbent for the treatment of wastewater in dye industries.[4,20−23] Actually, polymers have some advantages, like a large number of adsorbent sites, good environmental stability, durability, etc., over small molecules. We have chosen polyaniline (PANI), one of the conjugated polymers due to its easy synthesis, low production cost, eco-friendliness, good environmental and thermal stability, simple doping/dedoping chemistry, and nontoxic nature.[24−26] However, synthesis of PANI nanstructure,

Received: March 2, 2019
Accepted: June 14, 2019
Published: June 14, 2019

DOI: 10.1021/acsapm.9b00199
ACS Appl. Polym. Mater. 2019, 1, 1624−1633

Scheme 1. Schematic Presentation of PANI Nanostructures Synthesis

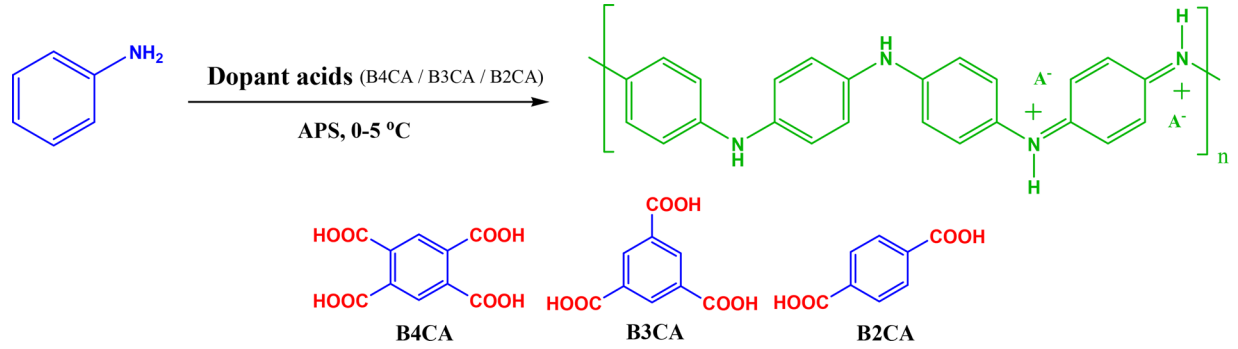

particularly nanotube without using any an external template is a really challenging task. Polyaniline nanotubes (PNTs) have many advantages over carbon nanotubes (CNTs). PNT is economically cheap and easy to synthesize; apart from this it has large specific surface areas, a hollow tube and porous structure that makes excellent adsorbent material. As PNTs are high specific surface area (SSA) and hollow tubular in nature, enough adsorption sites for wastewater treatment would be available owing to the presence of the large number of amine and imine groups and we may expect PNTs as good materials for water purification.[9,27] Although the SSA of activated carbon is higher than that of PNTs, activated carbon has several disadvantages like flammability and difficult reuse for dye uptake application from polluted water.[28,29]

Recently, Wang et al. prepared kapok fiber oriented polyaniline and used it as an adsorbent for sulfonated dye removal with maximum adsorbed capacity ~190 mg/g after 4 h.[10] Xu et al. reported an organic/inorganic hybrid material of polyaniline/α-zirconium phosphate (PANI/αZrP) and showed maximum adsorption capacity 377 mg/g.[30] Patra et al. reported Potash Alum-doped polyaniline for anionic dye removable from aqueous solution.[31] Ayad et al. designed a polyaniline nanotube base/silica composite as a powdered form for the removal of cationic dye.[32] Ding et al. revealed a membrane combining cellulose acetate (CA) nanofibers and a fluorinated polybenzoxazine (F-PBZ) layer incorporating silica nanoparticles for oil/water separation.[33] Men et al. incorporated polyaniline into cotton fabrics via a facile vapor phase deposition process, and composites were used for oil/water separation.[18] All these above-mentioned studies have utilized the hard templated polyaniline nanostructure for dye adsorption. So far, none has utilized directly the polyaniline nanostructure prepared by the soft template method for dye adsorption as well as oil/water separation, though the soft template method is simple, cost-effective, and stable for large scale synthesis of the PANI nanostructure. Therefore, the present work aims to develop the synthesis of a high aspect ratio polyaniline nanotube and subsequently to apply these fibers to dye separation from wastewater as well as oil separation from oil/water mixture with good efficiency, stability, and easy reuse.

In this article, we have reported a facile method for PANI nanostructure preparation in large scale by the chemical polymerization method as well as for wastewater treatment and oil/water separation. Three organic dopant acids (B4CA, B3CA, and B2CA) with different numbers of −COOH groups have been selected for the synthesis of nanostructures. After characterization with FTIR, UV−vis, FESEM, TEM, TGA, etc., synthesized PANI nanostructures are utilized for dye adsorption studies. Different dyes are used like Congo red (CR), Eriochrome Black T (EBT), Methyl orange (MO), Indigo carmine (IC), *N*,*N*′-bis(4-benzosulfonic acid)perylene-3,4,9,10-tetracarboxylbisimide (PRSA), Methylene blue (MB), and Crystal violet (CV) for the dye adsorption study and toluene, kerosene, diesel, hexane, and petroleum ether are used for the oil/water separation study. Indigo carmine (IC) is chosen as the model dye for the detailed adsorption study. The prepared B4CAP nanostructure shows good recyclable property for adsorption of colored dye molecules by simple washing with diluted ammonia and acid solution. The dye separation study has indicated that the recyclable PANI nanotubes may be used as a desirable adsorbent for environmental remediation in bulk amounts. Furthermore, the prepared matrix is also applicable for oil/water separation from a mixture.

2. EXPERIMENTAL SECTION

2.1. Materials. 1,2,4,5-Benzenetetracarboxylic acid (B4CA), 1,3,5-benzenetricarboxylic acid (B3CA), 1,4-benzenedicarboxylic acid (B2CA), and ammonium persulfate [$(NH_4)_2S_2O_8$ (APS)] were purchased from Sigma-Aldrich and used without further purification. Merck Chemicals provided aniline (distilled under reduced pressure and stored at 5 °C in a dark place before use), and hydrochloric (HCl) acid was purchased from commercial sources as analytical pure reagents. All dye molecules were purchased from local chemical companies. All solutions were prepared in deionized water (18 MΩ cm, Millipore Milli Q water system).

2.2. Instrumentation. *2.2.1. Microscopy.* The surface morphology of synthesized composites was observed by FESEM. A small amount of samples was dispersed in water by sonication and was drop casted on a glass coverslip and then dried at room temperature. A JEOL, JSM 6700F instrument operating at 5 kV was used for imaging. Samples were coated with platinum for 90 s to reduce the surface potential. Transmission electron microscopy (TEM) was performed with an HRTEM (JEOL, 2010EX) instrument at an accelerating voltage of 200 kV. The water dispersed composite samples were drop casted over a 200 mesh Cu-grid coated with a holey carbon supported film, and images were taken using a CCD.

2.2.2. Spectroscopy. UV−vis studies of PANI composite samples were recorded using a Hewlett-Packard UV−vis spectrophotometer, model 8453, in a 1.0 cm path length quartz cell. Samples were dispersed in water prior to investigation of the sample under UV−vis measurement. FTIR studies of PANI samples were done using an FTIR-8400S (Shimadzu) instrument by making KBr pellets.

2.2.3. Structural Study. XRD measurements of PANI composite samples were performed using a Bruker AXS diffractometer (D8 advance), a generator voltage of 40 kV, and a current of 40 mA with Cu Kα radiation (λ = 1.54 Å). Samples were scanned in 2θ = 10−40° ranges with a scan rate of 0.4 s per step with a step width of 0.02°. Thermogravimetric analysis (TGA) of B4CAP was performed with a TA thermal analysis instrument with a temperature range from 25 to 800 °C at a heating rate of 10 °C/min under a nitrogen environment.

DOI: 10.1021/acsapm.9b00199
ACS Appl. Polym. Mater. 2019, 1, 1624−1633

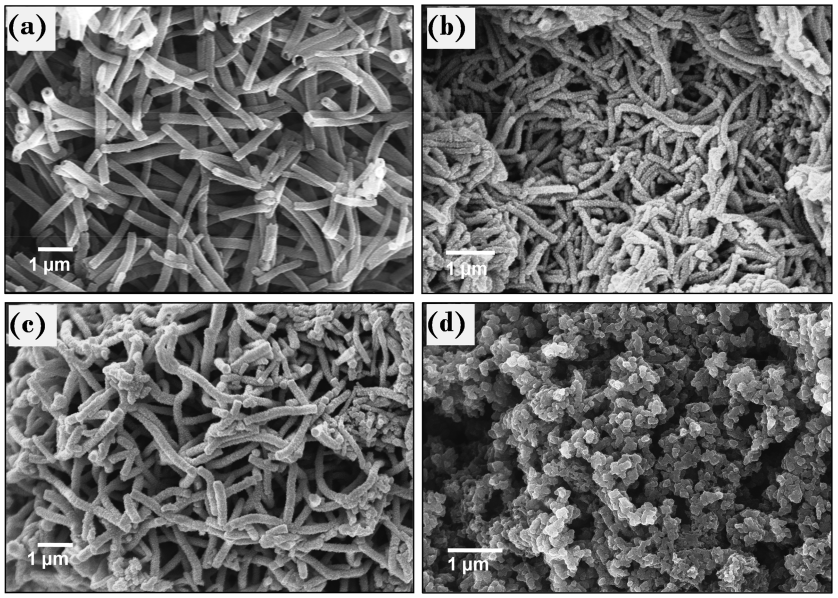

Figure 1. FESEM images of synthesized PANI nanostructures namely (a) B4CAP, (b) B3CAP, (c) B2CAP, and (d) HDP.

BET surface area measurements were performed using a Quantachrome Autosorb-1C to get the surface area of the PANI matrix.

2.3. Preparation of B2CAP, B3CAP, and B4CAP. The synthesis procedure for PANI nanostructures was followed by our early report (Scheme 1).[34,35] In the typical reaction, the required amount of different dopant acids (like B2CA, B3CA, and B4CA) was dissolved in 15 mL of water with continuous stirring at room temperature for the synthesis of PANI nanostructures, namely, B2CAP, B3CAP, and B4CAP (Table S1). Aniline (100 μL, 1.02 g/cm^3, 1.1 mmol) was added to each solution with an additional 1 h of vigorous stirring. After the reaction temperature was cooled to 10 °C, an aqueous solution of APS was added drop by drop to the reaction mixture. Immediately, the solution color changed from yellow to brown and the mixture was allowed to stand at 0−5 °C temperature for 24 h. The resulting deep green color precipitate was washed with water followed by methanol several times to remove oligomers and excess APS from the reaction mixture. Finally, the product was dried in a vacuum oven at 60 °C to get PANI nanostructures in powdered form.

2.4. Adsorption Investigation. Dye adsorption studies were carried out by the batch reaction technique in glass vials. The dye concentration of different batch reactors was determined colorimetrically by measuring absorbance maxima (λ_{max} 611, 502, 540, 464 nm for IC, PRSA, EBT, and MO) of the dyes using the UV−vis spectrometer. Concentration of dye in solution at different batch reactors (different times, different adsorbent dose, etc.) was determined by Beer−Lambert's law expression. For the kinetic study, 3.5 mg of PANI nanostructures was added to 20 mL of dye solution. An aliquot of sample was taken out from reaction mixture with an appropriate time interval. Supernatant liquid was separated by centrifuging at 5000 rpm for 5 min, and adsorption of supernatant liquid was determined by UV−vis spectroscopy. The amount of dye adsorbed was calculated by eq 1.[2,20,36]

$$Q_t = \frac{(C_0 - C_t}{m} \quad (1)$$

The dye removable percentage (% R) was calculated from eq 2[37,38]

$$R\% = \frac{(C_0 - C_t)}{C_0} \times 100 \quad (2)$$

where "C_0" and "C_t" were dye solution concentration (mg/L) at time "0" and "t" respectively, "V" was the total volume of solution (L), and "m" was the mass of PANI nanostructures (g).

2.5. Oil−Water Separation. The oil−water separation study was made from a toluene/water mixture, which was considered as a model mixture of oil/water for detailed study. In the typical experiment, a mixture of 5 mL of toluene and 5 mL of water was poured into a column packed with PANI nanostructures solid materials. The oil part was marked by red color with Sudan IV dye and the water part remained transparent colorless. Once the oil/water mixture was poured into the column, the high density water part went to the bottom of the column and the oil part was on top. After some time, the water part (colorless) passed through the PANI nanostructure; however, the oil part did not pass through it. The separation efficiency ($Q_{separation}$) of a variety of oils was expressed by eq 3[39]

$$Q_{sepeartion} = \frac{m_{seperation}}{m_{initial}} \times 100 \quad (3)$$

where "$m_{separation}$" and "$m_{initial}$" were the weight of water after each separation (g) and weight of water initially (g) in the oil−water mixture.

3. RESULTS AND DISCUSSION

3.1. Morphological Study. FESEM images of different acid-doped PANI nanostructures are shown in Figure 1.

Table 1. PANI Nanostructures Nature and Adsorption Capacity

nanostructure	fiber nature	aspect ratio	dye uptake after a fixed time[a] (mg/g)
B4CAP	tube	∼115	300
B3CAP	tube	∼35	245
B2CAP	tube	∼20	230
HDP (control)	agglomerate		170

[a]After 90 min to get the equilibrium level.

Excellent fibrous-like morphologies are observed for B4CAP, B3CAP, and B2CAP composites and almost all B4CAP fibers are tube-like in nature. For comparison, HCl-doped polyaniline (HDP) that has been synthesized under identical conditions produces spherical agglomerate-like morphology. A careful observation of each nanostructure provides information about fiber diameter, length, and the nature of the fiber. The highest aspect ratio (length/diameter) is ∼115 for B4CAP nanostructures. Values of same ratio for B3CAP and B2CAP are ∼35 and

DOI: 10.1021/acsapm.9b00199
ACS Appl. Polym. Mater. 2019, 1, 1624−1633

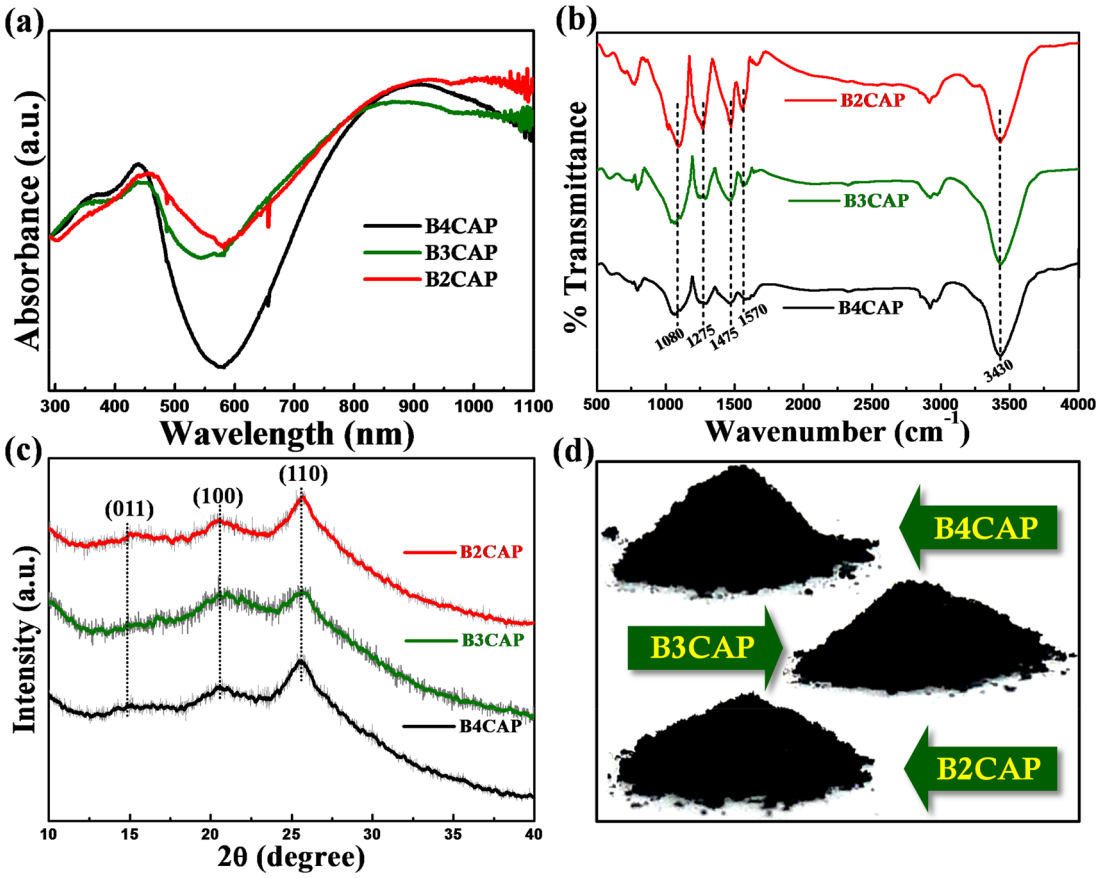

Figure 2. (a) UV−vis study (inset image for nanotube of PANI), (b) FTIR spectra, (c) powdered XRD pattern, and (d) digital image of solid large scale synthesized PANI nanostructures for B2CAP, B3CAP, and B4CAP.

~20, respectively (Table 1), indicating that these fibers have the same tube-like hollow pattern morphology as B4CAP. The fiber patterns of B4CAP are very uniform, with hollow tubes and high aspect ratios that may facilitate the adsorption of toxic dye present in an aqueous medium.

3.2. Spectroscopic Study. UV−vis spectra of the PANI nanostructures from disperse aqueous solution (Figure 2a) show three absorption peaks centered at ~350, 435, and 910 nm. Two peaks at ~350 and 435 nm are assigned to the $\pi-\pi^*$ and polaron$-\pi^*$ transitions of benzenoid rings, respectively. Another peak at ~910 nm with a free tail extendeing to the IR region is assigned to the π−polaron transition.[29,34] These three characteristic PANI peaks are present in the three B4CAP, B3CAP, and B2CAP nanostructures. It means that PANI chains remain in the emeraldine salt state in all nanostructures. The absorption intensity of the π−polaron transition (peak at ~880−910 nm) is sharp for B4CAP compared to the same in B3CAP and B2CAP, revealing the decrease of the conjugation length of PANI chains in the B3CAP and B2CAP nanostructures.

3.3. FTIR Study. To confirm the PANI formation in all nanostructures, an FTIR study was performed for B4CAP, B3CAP, and B2CAP composites (Figure 2b). The presence of stretching vibration bands at ~3430, 2930, 1620, 1570, 1475 1275, 1125, and 798 cm^{-1} reveals the PANI formation. The characteristic stretching bands at 3430 cm^{-1} for γN—H of the PANI chain, 2930 cm^{-1} for γC—H of the phenyl rings, 1620 cm^{-1} for γC═C of the quinoid rings, 1440 cm^{-1} for γC═C of the benzenoid rings, 1297 cm^{-1} for γC—N of the secondary aromatic amine, 1125 cm^{-1} for γC—H aromatic in-plane, and 798 cm^{-1} γC—H aromatic out-of-plane deformation for 1,4 disubstituted benzene prove PANI formation in the nanostructures.[30,34,35,40]

3.4. XRD Study. Powder X-ray diffraction (XRD) patterns of B4CAP, B3CAP, and B2CAP samples are shown in Figure 2c. The XRD patterns show peaks at $2\theta \approx 15°$, 20.3°, and 25.6° for (011), (100), and (110) planes, revealing the small crystalline nature of PANI composites. The peak responses at 2θ = 20.3° and 25.6° are for periodicity in parallel and perpendicular directions to the PANI chain, respectively.[29,41] The peak at 25.6° corresponds to *d*-spacing ~3.48 Å for the face-to-face interaction of phenyl rings of PANI chains.[34] The highest intensity peak at 25.6° is observed for B4CAP, suggesting a greater extent of $\pi-\pi$ staking of the polymer chain in B4CAP than in the other two nanostructures.

3.5. TGA Study. The thermogravimetric analysis (TGA) of the B4CAP matrix was done under a N_2 atmosphere from 25 to 800 °C (Figure S1). Nanostructures show a three-step weight loss behavior. The first weight loss at ~100 °C relates to the presence of moisture in samples. The second and third weight losses at ~250 and 535 °C are for dedoping of dopant acids and decomposition of the polymer main chain, respectively.[42,43] The nature of the TGA curve shows good thermal stability of the B4CAP matrix due to the good packing density of the B4CAP nanostructures.

3.6. Dye Adsorption Study. Currently, many industries are widely using several dyes and these are directly drained into water in such a way that they contaminate not only rivers, ponds,

DOI: 10.1021/acsapm.9b00199
ACS Appl. Polym. Mater. 2019, 1, 1624−1633

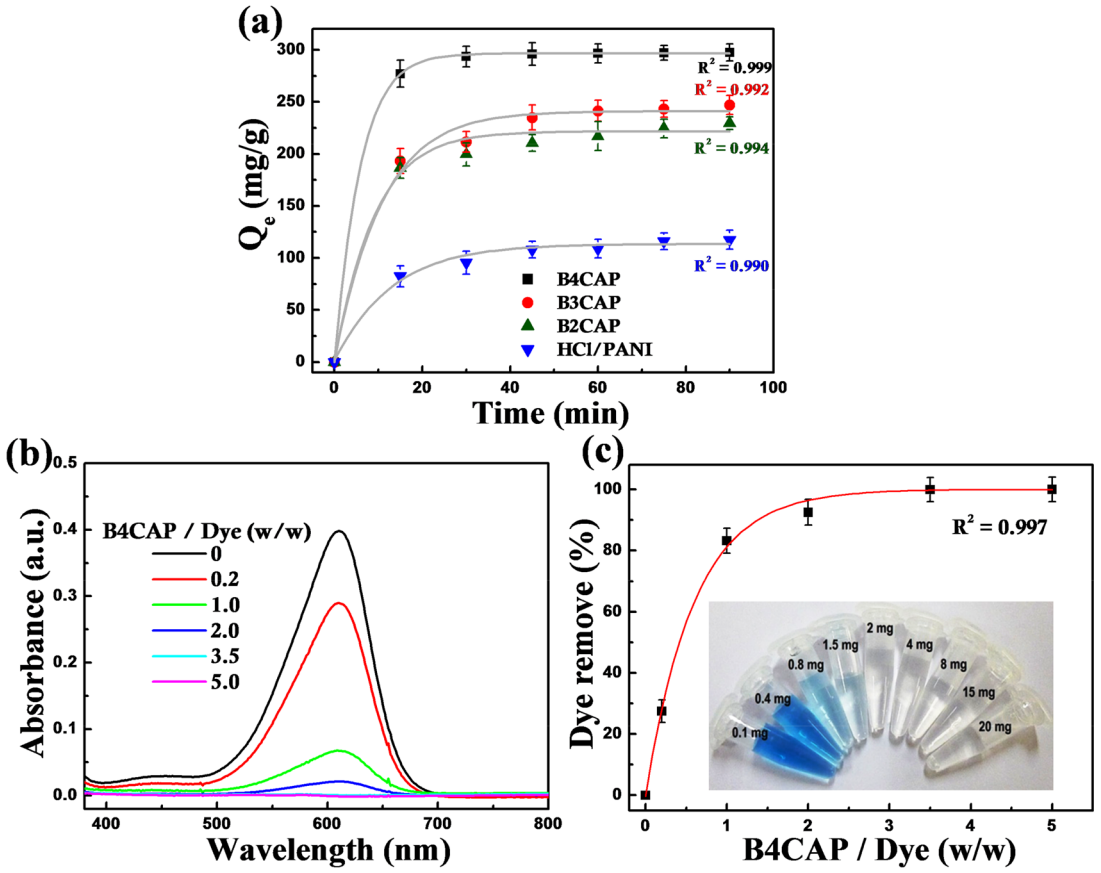

Figure 3. (a) Dye adsorption studies by different PANI matrixes at room temperature with the same PANI to dye (w/w) ratio. (b) UV−vis spectra of IC dye with different adsorbent doses. (c) Corresponding plot for dye removable % vs adsorbent dose to amount of dye (w/w) ratio.

Scheme 2. Chemical Structure of Different Dye Molecules Used in the Adsorption Studies

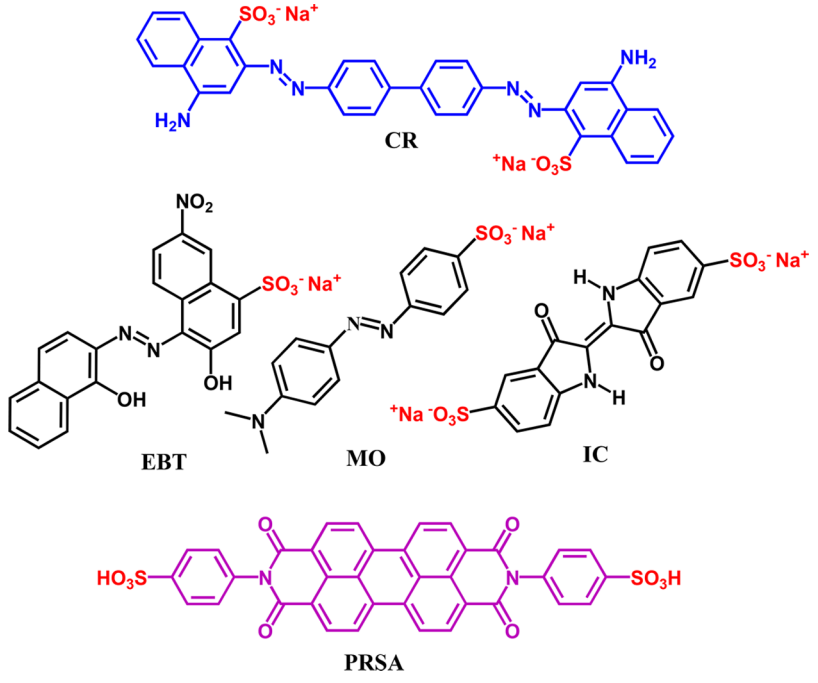

and wells but they also pollute the Earth. Separation of dye from the wastewater has received deep attention from the environmental point of view.[1,2,5] With the aim of finding an efficient material for dye removal, we have judiciously picked up three aromatic acid-doped PANI nanotubes (B4CAP, B3CAP, and B2CAP, Figure 2d) for dye removal study and HCl-doped polyaniline (HDP) has been used for the control experiment. Indigo carmine (IC) dye is chosen as a model dye for detailed

DOI: 10.1021/acsapm.9b00199
ACS Appl. Polym. Mater. 2019, 1, 1624−1633

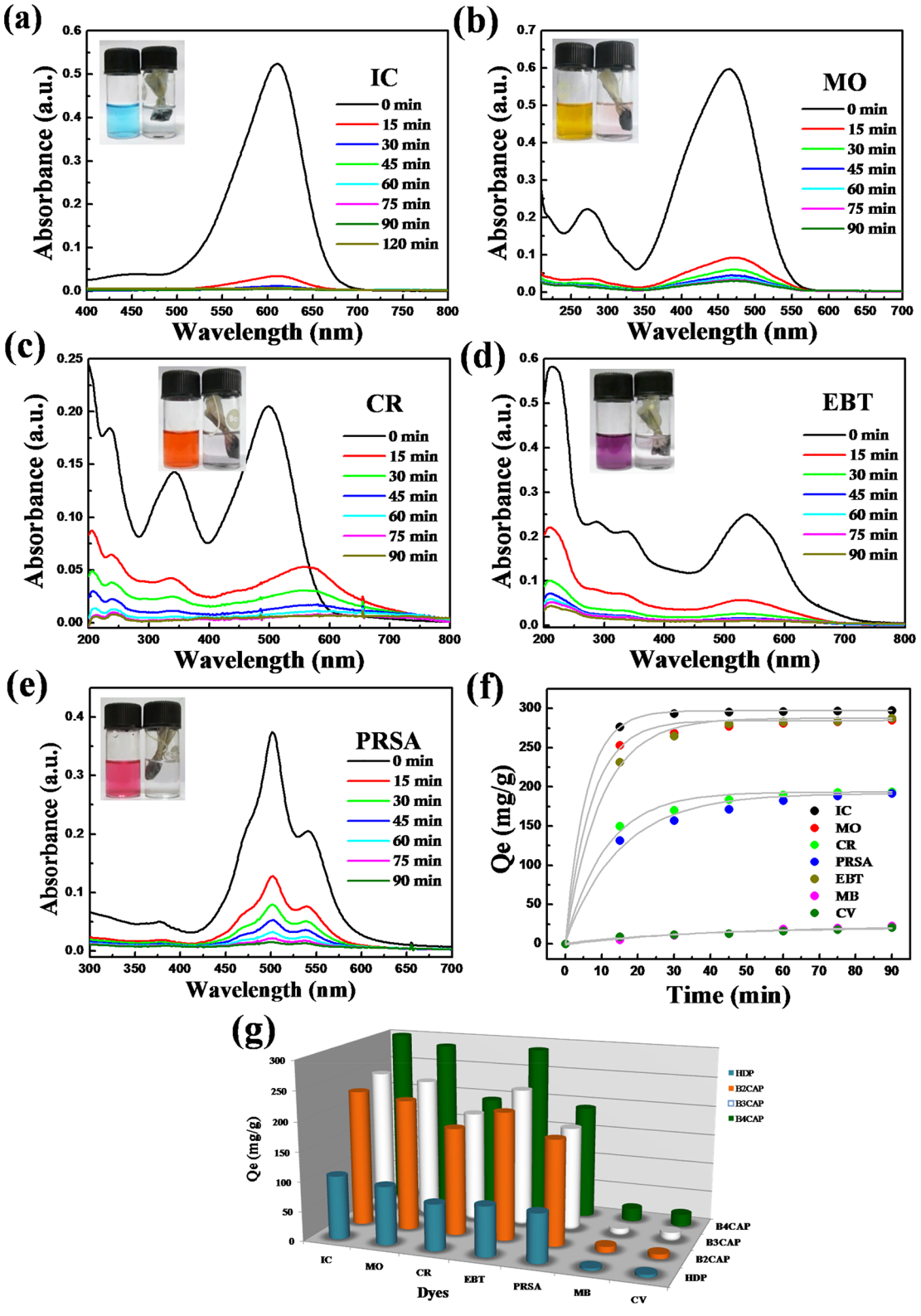

Figure 4. UV−vis spectra monitored at different times in the presence of B4CAP nanostructure dispersed in aqueous medium: (a) IC, (b) MO, (c) CR, (d) EBT, and (e) PRSA. (f) Rate of dye uptake with all the selected dyes with B4CAP. (g) Plot for the rate of dye uptake of different dye molecules with PANI nanostructures (B4CAP, B3CAP, B2CAP, and HDP).

adsorption study at room temperature (Figure 3). UV−vis spectra for dye adsorption for these three polymers are shown in Figure S2.

Among four PANI composites, B4CAP has shown higher dye uptake capacity and it is ∼300 mg/g to IC compared with capacities of B3CAP, B2CAP, and HDP (∼245, ∼230, and ∼107 mg/g respectively) (Table 1). The reason can be explained from the aspect ratio of the nanotubes. The aspect ratio of the B4CAP fiber is higher and every fiber shows uniform hollow tube-like morphology (Figure 1a and S3), which has

DOI: 10.1021/acsapm.9b00199
ACS Appl. Polym. Mater. 2019, 1, 1624−1633

Table 2. Different Dye Molecule Specification and Adsorption Efficiency

dye	molar mass (g/mol)	λ_{max} (nm)	dye nature	adsorption (mg/g)
IC	466.36	609	anionic	300
MO	327.33	464	anionic	285
CR	696.68	499	anionic	194
EBT	461.38	535	anionic	288
PRSA	702.67	502	anionic	192
MB	319.85	664	cationic	22.6
CV	407.97	588	cationic	21.1

produced more specific surface area (SSA) for dye adsorption than that of the B3CAP and B2CAP fiber along with the agglomerate morphology of HDP. The higher SSA of B4CAP (83.93 m^2/g) compared to the same of B3CAP (41.5 m^2/g) and B2CAP (15.7 m^2/g) is also confirmed by BET studies (Figure S4). In the adsorption or separation study, the adsorption capacity (Q_e) is another important parameter. To obtain the optimum adsorption capacity between the adsorbent dosage and the the amount of dye, we have changed the adsorbent mass (PANI) and kept the dye concentration (mg/L) constant. The characteristic UV−vis absorption maxima of the IC dye (λ = 611 nm) decreases gradually with increasing the amount of B4CAP nanostructure (Figure 3b). With an increasing PANI (adsorbent dose) to dye (w/w) ratio, the dye removable percentage increases. After a certain ratio of adsorbent dose to dye (w/w), it becomes 100% and it is considered the optimum condition for the adsorbent dose. It is found from Figure 3c that the optimum condition for the adsorbent dose (B4CAP) to IC ratio is 3.5:1 (w/w).

Various types of toxic dyes are present in industrial wastewater. To apply our synthesized PANI nanostructure in a broad sense of applications, seven different dyes have been chosen in the adsorption or separation studies, these are Congo red (CR), Eriochrome Black T (EBT), Methyl orange (MO), Indigo carmine (IC), PRSA, Methylene blue (MB), and Crystal violet (CV) (Scheme 2).

The amount of dye uptake of B4CAP has been monitored by UV−vis absorption spectroscopy at different time intervals (Figure 4a−e). It has been found that the dye uptake rate of the B4CAP nanostructure depends on the charge as well as the size of the dye molecule. Anionic dye molecules (like IC^-, CR^-, MO^-, EBT^-, $PRSA^-$, etc.) are adsorbed more rapidly than cationic dye molecules (MB^+, CV^+, etc., Figure S5). The charge of the dye molecule is not the only factor; molecular size also plays an important role on the rate of dye uptake. As shown in Figure 4f, the rate of IC dye uptake is more than that of other selected dyes, calculated from the UV−vis study of selected dyes with different time intervals. It is possibly due to the smaller size as well as the presence of two negative charges (two sulfonated unit) in the IC dye molecule. Though the size of EBT and MO are comparable to IC, only one negative charge (one sulfonated unit) on each molecule results from the slower rate of adsorption than that of the IC dye molecule. PRSA and CR have two negative charges (two sulfonated unit), these are bigger in size than other selected dye molecules. The larger size causes lower diffusion of dye in solution,and as a result, slow rates of dye uptake are observed. As MB and CV are positively charged dye molecules, they are adsorbed at slower rates.[44] The rate of dye adsorption follows the order IC > MO ⩾ EBT > CR ⩾ PRSA > MB ≈ CV (Table 2). Rates of dye uptake of seven dyes with all nanostructures have been investigated, and the results are summarized in Figure 4g. The mechanism of dye adsorption on the PANI surface occurs via electrostatic interaction between dye molecules and the PANI surface, as shown in Figure S6 (Supporting Information). The sulfonated ($-SO_3^-$) dye molecules electrostatically interact with the positively charged backbone of PANI (emeraldine salt), leading to the adsorption of various sulfonated dyes on the PANI surface. For the dye adsorption study, B4CAP is the best PANI nanostructure among four. The effect of pH for adsorption has also been observed (Figure S7). With increasing pH from neutral to basic pH, the adsorption capacity is sharply decreased. Decreasing the pH from neutral to acidic, the adsorption capacity little decreases. Therefore, the maximum adsorption capacity is observed at

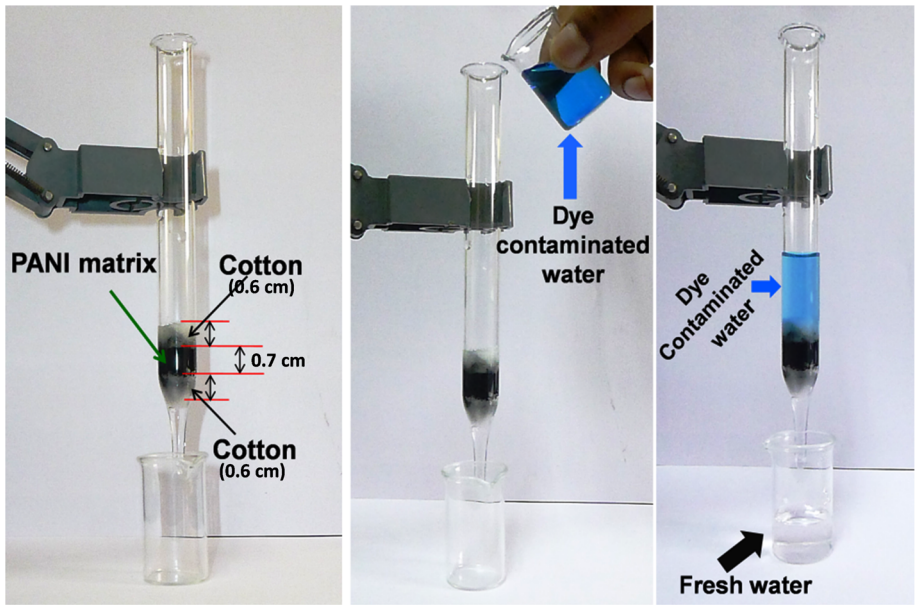

Figure 5. Presentation of dye separation process (IC as a model dye, ~5 mg/mL) on a large scale by a glass column packed with B4CAP nanostructures sandwiched between cotton layers.

DOI: 10.1021/acsapm.9b00199
ACS Appl. Polym. Mater. 2019, 1, 1624−1633

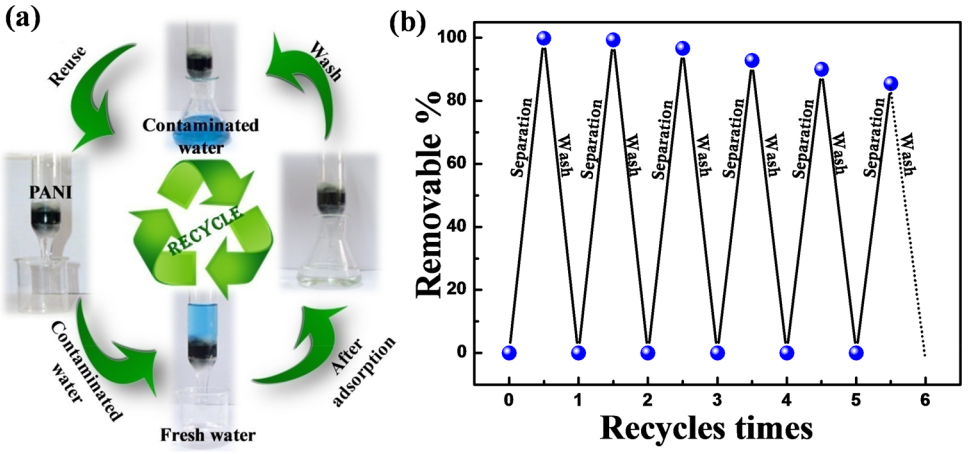

Figure 6. Recyclability study. (a) Schematic presentation. (b) Plot between removable percent versus reusable times of PANI nanostructure for IC dye (model selected dye) separation.

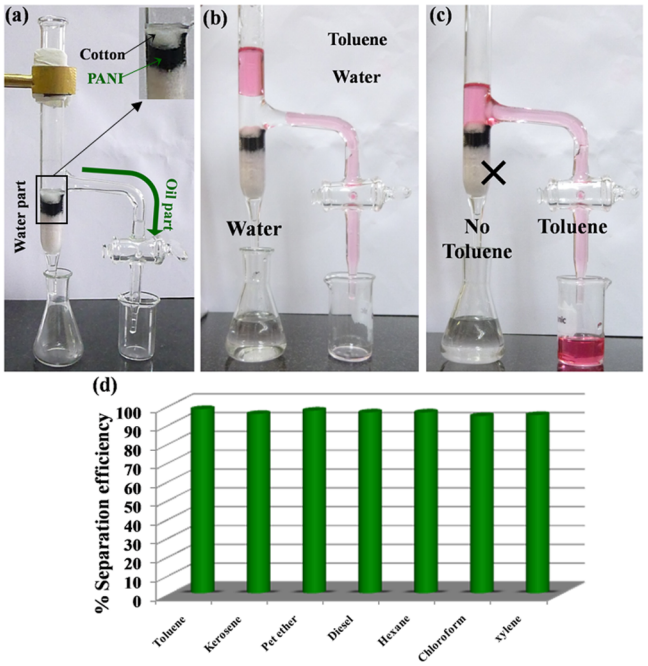

Figure 7. Schematic presentation of (a) column design packed with B4CAP nanotubes between two cotton layers, (b) oil/water separation from a mixture, (c) oil and water collection after 6 h by two different containers, and (d) separation efficiency of different oil form oil/water mixtures at room temperature by a column packed with B4CAP.

neutral pH (pH = 7). To show the performances of B4CAP nanostructures, an aqueous solution of IC dye (typically 5 mg/mL) has been passed through the B4CAP matrix sandwiched between cotton layers, as pictorially represented in Figure 5. IC dyes are adsorbed on the surface of B4CAP nanatubes and fresh water (checked by UV-vis spectra) is stored at the bottom. Furthermore, we have compared maximum dye adsorption capacity of our PANI matrix with some reported polyaniline related work (Table S2, Supporting Information)

3.7. Recyclability Study of B4CAP Nanostructure. Recyclability or regeneration is an important factor from the practical application point of view.[45,46] After dye adsorption, solid PANI has been properly washed with diluted NH_3 solution followed by acid and water for the next adsorption study. Desorption of dye from PANI nanostructures has been monitored by UV−vis absorption spectroscopy. Figure 6 shows the recyclable study results of IC dye (model dye), and after five consecutive adsorption cycles, the B4CAP has showed the retention of 85% efficiency. The tube-like morphology of B4CAP remains intact even after fifth cycle of dye adsorption studies, as evidenced from the FESEM investigation (Figure S8)

3.8. Oil−Water Separation Study. Oil/water separation is an area of high impact study in recent days from different points of view like industrial benefits, green environment, etc. For the oil/water separation study, a column packed with B4CAP matrix sandwiched between two cotton layers has been prepared (Figure 7). Demonstration of the separation has been performed by using toluene, kerosene, petroleum ether, diesel, hexane, chloroform, and xylene as the oil part. Initially, the toluene/water mixture has been demonstrated as model oil/water mixture for our experiment. After pouring the toluene/water mixture into the column, the water part (transparent part) of the mixture easily passes through the B4CAP packed column by gravimetric force, whereas the toluene part (oil part marked as pinkish color with sudhan IV dye) cannot pass (Figure 7c). The strong hydrophilic nature of synthesized PANI due to the presence of a large number of amine and imine groups in the PANI chain dislikes the oil part (i.e., toluene). The percentage of separation efficiency (% R) has been calculated for each mixture by following eq 3. The calculated % R values for toluene, kerosene, petroleum ether, diesel, hexane, chloroform, and xylene are 97.8, 95.2, 97.0, 96.0, 96.1, 94.1, and 94.9, respectively (Figure 7d). Therefore, the separation procedure is highly energy efficient because the methodology is solely gravity-driven; no external force or high voltage is required for separation.

4. CONCLUSION

We have successfully demonstrated PANI nanotubes in large scale to develop a method for adsorption of dye from a water contaminated dye solution as well as separation of oil form an oil/water mixture. The aspect ratio of PANI fibers depends on the nature of the dopant acid used. The maximum aspect ratio has been achieved for the B4CAP nanotube, where B4CA is the dopant acid. Synthesized PANI nanostructures are able to adsorb anionic dye molecules in an aqueous solution with maximum adsorption efficiency ~300 mg/g. The dye adsorption ability of PANI nanostructure is also controlled by tuning the aspect ratio of the PANI fibers. The rate of dye uptake

DOI: 10.1021/acsapm.9b00199
ACS Appl. Polym. Mater. 2019, 1, 1624−1633

significantly depends on the size as well as the charge of the dye molecule. PANI shows good reuse property upon treatment with dilute ammonia for dye adsorption up to several cycles. The hydrophilic property of the PANI nanostructure facilitates oil/water separation from a mixture by gravitational means and, thus, is energetically favorable. We believe that our synthesized PANI nanotubes will be useful for numerous applications, including industrial dye adsorption, wastewater treatment, fuel purification, and separation of commercially relevant emulsions.

■ ASSOCIATED CONTENT

Supporting Information

The Supporting Information is available free of charge on the ACS Publications website at DOI: 10.1021/acsapm.9b00199.

Preparation of PANI matrix, synthesis of HDP and PRSA, TGA study of B4CAP, UV−vis change with time, adsorbent type etc., FESEM and TEM images of B4CAP, BET adsorption isotherms, effect of pH on dye adsorption, morphology of B4CAP matrix before and after adsorption, comparison of literature data (PDF)

■ AUTHOR INFORMATION

Corresponding Author

*E-mail: psusm2@iacs.res.in.

ORCID

Sanjoy Mondal: 0000-0002-4391-6356

Utpal Rana: 0000-0001-5026-1303

Sudip Malik: 0000-0001-5358-5653

Notes

The authors declare no competing financial interest.

■ ACKNOWLEDGMENTS

Dr. Malik acknowledges CSIR, INDIA (project no. 01(2875)/17/EMR-II) for the financial support. Dr. S. Mondal. acknowledges to CSIR, New Delhi, India for the fellowship. P. Das is thankful to DST INSPIRE, India for the fellowship.

■ REFERENCES

(1) Ali, I. New Generation Adsorbents for Water Treatment. *Chem. Rev.* **2012**, *112*, 5073−5091.

(2) Ma, J.; Yu, F.; Zhou, L.; Jin, L.; Yang, M.; Luan, J.; Tang, Y.; Fan, H.; Yuan, Z.; Chen, J. Enhanced Adsorptive Removal of Methyl Orange and Methylene Blue from Aqueous Solution by Alkali-Activated Multiwalled Carbon Nanotubes. *ACS Appl. Mater. Interfaces* **2012**, *4*, 5749−5760.

(3) Unuabonah, E. I.; Günter, C.; Weber, J.; Lubahn, S.; Taubert, A. Hybrid Clay: A New Highly Efficient Adsorbent for Water Treatment. *ACS Sustainable Chem. Eng.* **2013**, *1*, 966−973.

(4) Liu, L.; Gao, Z. Y.; Su, X. P.; Chen, X.; Jiang, L.; Yao, J. M. Adsorption Removal of Dyes from Single and Binary Solutions Using a Cellulose-Based Bioadsorbent. *ACS Sustainable Chem. Eng.* **2015**, *3*, 432−442.

(5) Mathieu-Denoncourt, J.; Martyniuk, C. J.; de Solla, S. R.; Balakrishnan, V. K.; Langlois, V. r. S. Sediment Contaminated with the Azo Dye Disperse Yellow 7 Alters Cellular Stress-and Androgen-Related Transcription in Silurana Tropicalis Larvae. *Environ. Sci. Technol.* **2014**, *48*, 2952−2961.

(6) Midya, L.; Das, R.; Bhaumik, M.; Sarkar, T.; Maity, A.; Pal, S. Removal of Toxic Pollutants from Aqueous Media using Poly (vinyl imidazole) Crosslinked Chitosan Synthesised Through Microwave Assisted Technique. *J. Colloid Interface Sci.* **2019**, *542*, 187−197.

(7) Zhu, X.; Liu, Y.; Zhou, C.; Zhang, S.; Chen, J. Novel and High-Performance Magnetic Carbon Composite Prepared from Waste Hydrochar for Dye Removal. *ACS Sustainable Chem. Eng.* **2014**, *2*, 969−977.

(8) Dou, X.; Li, P.; Zhang, D.; Feng, C.-L. C 2-Symmetric Benzene-Based Hydrogels with Unique Layered Structures for Controllable Organic Dye Adsorption. *Soft Matter* **2012**, *8*, 3231−3238.

(9) Mahanta, D.; Madras, G.; Radhakrishnan, S.; Patil, S. Adsorption and Desorption Kinetics of Anionic Dyes on Doped Polyaniline. *J. Phys. Chem. B* **2009**, *113*, 2293−2299.

(10) Zheng, Y.; Liu, Y.; Wang, A. Kapok Fiber Oriented Polyaniline for Removal of Sulfonated Dyes. *Ind. Eng. Chem. Res.* **2012**, *51*, 10079−10087.

(11) Cheng, N.; Hu, Q.; Guo, Y.-X.; Wang, Y.; Yu, L. Efficient and Selective Removal of Dyes Using Imidazolium-Based Supramolecular Gels. *ACS Appl. Mater. Interfaces* **2015**, *7*, 10258−10265.

(12) Sukul, P. K.; Malik, S. Removal of Toxic Dyes from Aqueous Medium Using Adenine Based Bicomponent Hydrogel. *RSC Adv.* **2013**, *3*, 1902−1915.

(13) Haque, E.; Jun, J. W.; Jhung, S. H. Adsorptive Removal of Methyl Orange and Methylene Blue from Aqueous Solution with a Metal-Organic Framework Material, Iron Terephthalate (Mof-235). *J. Hazard. Mater.* **2011**, *185*, 507−511.

(14) Sreeprasad, T. S.; Maliyekkal, S. M.; Lisha, K. P.; Pradeep, T. Reduced Graphene Oxide−Metal/Metal Oxide Composites: Facile Synthesis and Application in Water Purification. *J. Hazard. Mater.* **2011**, *186*, 921−931.

(15) Singh, K. P.; Mohan, D.; Sinha, S.; Tondon, G.; Gosh, D. Color Removal from Wastewater Using Low-Cost Activated Carbon Derived from Agricultural Waste Material. *Ind. Eng. Chem. Res.* **2003**, *42*, 1965−1976.

(16) Zhu, T.; Chen, J. S.; Lou, X. W. Highly Efficient Removal of Organic Dyes from Waste Water Using Hierarchical NiO Spheres with High Surface Area. *J. Phys. Chem. C* **2012**, *116*, 6873−6878.

(17) Yan, Y.; Zhang, M.; Gong, K.; Su, L.; Guo, Z.; Mao, L. Adsorption of Methylene Blue Dye onto Carbon Nanotubes: A Route to an Electrochemically Functional Nanostructure and Its Layer-by-Layer Assembled Nanocomposite. *Chem. Mater.* **2005**, *17*, 3457−3463.

(18) Zhou, X.; Zhang, Z.; Xu, X.; Guo, F.; Zhu, X.; Men, X.; Ge, B. Robust and Durable Superhydrophobic Cotton Fabrics for Oil/Water Separation. *ACS Appl. Mater. Interfaces* **2013**, *5*, 7208−7214.

(19) Vilela, D.; Parmar, J.; Zeng, Y.; Zhao, Y.; Sanchez, S. Graphene-Based Microbots for Toxic Heavy Metal Removal and Recovery from Water. *Nano Lett.* **2016**, *16*, 2860−2866.

(20) Wang, L.; Wang, A. Adsorption Characteristics of Congo Red onto the Chitosan/Montmorillonite Nanocomposite. *J. Hazard. Mater.* **2007**, *147*, 979−985.

(21) Crini, G. Recent Developments in Polysaccharide-Based Materials Used as Adsorbents in Wastewater Treatment. *Prog. Polym. Sci.* **2005**, *30*, 38−70.

(22) Crini, G.; Badot, P.-M. Application of Chitosan, a Natural Aminopolysaccharide, for Dye Removal from Aqueous Solutions by Adsorption Processes Using Batch Studies: A Review of Recent Literature. *Prog. Polym. Sci.* **2008**, *33*, 399−447.

(23) Blackburn, R. S. Natural Polysaccharides and Their Interactions with Dye Molecules: Applications in Effluent Treatment. *Environ. Sci. Technol.* **2004**, *38*, 4905−4909.

(24) Mondal, S.; Rana, U.; Malik, S. Graphene Quantum Dot-Doped Polyaniline Nanofiber as High Performance Supercapacitor Electrode Materials. *Chem. Commun.* **2015**, *51*, 12365−12368.

(25) Rana, U.; Malik, S. Graphene Oxide/Polyaniline Nanostructures: Transformation of 2d Sheet to 1d Nanotube and in Situ Reduction. *Chem. Commun.* **2012**, *48*, 10862−10864.

(26) Rana, U.; Chakrabarti, K.; Malik, S. *In Situ* Preparation of Fluorescent Polyaniline Nanotubes Doped with Perylene Tetracarboxylic Acids. *J. Mater. Chem.* **2011**, *21*, 11098−11100.

(27) Mahto, T. K.; Chandra, S.; Haldar, C.; Sahu, S. K. Kinetic and Thermodynamic Study of Polyaniline Functionalized Magnetic Mesoporous Silica for Magnetic Field Guided Dye Adsorption. *RSC Adv.* **2015**, *5*, 47909−47919.

(28) Malik, P. Dye Removal from Wastewater Using Activated Carbon Developed from Sawdust: Adsorption Equilibrium and Kinetics. *J. Hazard. Mater.* **2004**, *113*, 81−88.
(29) Namasivayam, C.; Kavitha, D. Removal of Congo Red from Water by Adsorption onto Activated Carbon Prepared from Coir Pith, an Agricultural Solid Waste. *Dyes Pigm.* **2002**, *54*, 47−58.
(30) Wang, L.; Wu, X.-L.; Xu, W.-H.; Huang, X.-J.; Liu, J.-H.; Xu, A.-W. Stable Organic−Inorganic Hybrid of Polyaniline/A-Zirconium Phosphate for Efficient Removal of Organic Pollutants in Water Environment. *ACS Appl. Mater. Interfaces* **2012**, *4*, 2686−2692.
(31) Patra, B. N.; Majhi, D. Removal of Anionic Dyes from Water by Potash Alum Doped Polyaniline: Investigation of Kinetics and Thermodynamic Parameters of Adsorption. *J. Phys. Chem. B* **2015**, *119*, 8154−8164.
(32) Ayad, M. M.; El-Nasr, A. A.; Stejskal, J. Kinetics and Isotherm Studies of Methylene Blue Adsorption onto Polyaniline Nanotubes Base/Silica Composite. *J. Ind. Eng. Chem.* **2012**, *18*, 1964−1969.
(33) Shang, Y.; Si, Y.; Raza, A.; Yang, L.; Mao, X.; Ding, B.; Yu, J. An in Situ Polymerization Approach for the Synthesis of Superhydrophobic and Superoleophilic Nanofibrous Membranes for Oil−Water Separation. *Nanoscale* **2012**, *4*, 7847−7854.
(34) Rana, U.; Chakrabarti, K.; Malik, S. Benzene Tetracarboxylic Acid Doped Polyaniline Nanostructures: Morphological, Spectroscopic and Electrical Characterization. *J. Mater. Chem.* **2012**, *22*, 15665−15671.
(35) Rana, U.; Mondal, S.; Sannigrahi, J.; Sukul, P. K.; Amin, M. A.; Majumdar, S.; Malik, S. Aromatic Bi-, Tri-and Tetracarboxylic Acid Doped Polyaniline Nanotubes: Effect on Morphologies and Electrical Transport Properties. *J. Mater. Chem. C* **2014**, *2*, 3382−3389.
(36) Bahrudin, N. N.; Nawi, M. A.; Ismail, W. I. N. W. Physical and adsorptive characterizations of immobilized polyaniline for the removal of methyl orange dye. *Korean J. Chem. Eng.* **2018**, *35*, 1450−1461.
(37) Mahanta, D.; Madras, G.; Radhakrishnan, S.; Patil, S. Adsorption of Sulfonated Dyes by Polyaniline Emeraldine Salt and Its Kinetics. *J. Phys. Chem. B* **2008**, *112*, 10153−10157.
(38) Ghorai, S.; Sarkar, A.; Raoufi, M.; Panda, A. B.; Schönherr, H.; Pal, S. Enhanced Removal of Methylene Blue and Methyl Violet Dyes from Aqueous Solution Using a Nanocomposite of Hydrolyzed Polyacrylamide Grafted Xanthan Gum and Incorporated Nanosilica. *ACS Appl. Mater. Interfaces* **2014**, *6*, 4766−4777.
(39) Xu, B.; Wang, Y.; Jin, R.; Li, X.; Song, D.; Zhang, H.; Sun, Y. Magnetic Solid-Phase Extraction Based on Fe_3O_4@Polyaniline Particles Followed by Ultrafast Liquid Chromatography for Determination of Sudan Dyes in Environmental Water Samples. *Anal. Methods* **2015**, *7*, 1606−1614.
(40) Abdiryim, T.; Xiao-Gang, Z.; Jamal, R. Comparative Studies of Solid-State Synthesized Polyaniline Doped with Inorganic Acids. *Mater. Chem. Phys.* **2005**, *90*, 367−372.
(41) Lee, K.; Cho, S.; Park, S. H.; Heeger, A.; Lee, C.-W.; Lee, S.-H. *Nature* **2006**, *441*, 65−68.
(42) Zhang, L.; Long, Y.; Chen, Z.; Wan, M. The Effect of Hydrogen Bonding on Self-Assembled Polyaniline Nanostructures. *Adv. Funct. Mater.* **2004**, *14*, 693−698.
(43) Bourdo, S.; Li, Z.; Biris, A. S.; Watanabe, F.; Viswanathan, T.; Pavel, I. Structural, Electrical, and Thermal Behavior of Graphite-Polyaniline Composites with Increased Crystallinity. *Adv. Funct. Mater.* **2008**, *18*, 432−440.
(44) Ayad, M. M.; El-Nasr, A. A. Adsorption of Cationic Dye (Methylene Blue) from Water Using Polyaniline Nanotubes Base. *J. Phys. Chem. C* **2010**, *114*, 14377−14383.
(45) Zhou, L.; Gao, C.; Xu, W. Magnetic Dendritic Materials for Highly Efficient Adsorption of Dyes and Drugs. *ACS Appl. Mater. Interfaces* **2010**, *2*, 1483−1491.
(46) Ai, L.; Zeng, Y. Hierarchical Porous Nio Architectures as Highly Recyclable Adsorbents for Effective Removal of Organic Dye from Aqueous Solution. *Chem. Eng. J.* **2013**, *215*, 269−278.

DOI: 10.1021/acsapm.9b00199
ACS Appl. Polym. Mater. 2019, 1, 1624−1633